

of an isotropic temperature factor $U = 0.06 \text{ \AA}^2$, the ratio of the electron density of 0.03 Cl atom to that of a hydrogen is larger than 2 for $r = 0.2$. This result reinforces thus our hypothesis that pk(1) and pk(2) represent Cl atoms bonded to Cu.

In ClCu^{18} the Cl atoms form a tetragonal bipyramid with Cu-Cl distances of 2.29 Å in the basis and 2.91 Å along the pseudo-fourfold axis parallel to the layer plane. In ClCuMn , such a geometry cannot be realized for stochastically distributed Cu atoms as the coordination of the surrounding Mn atoms would be seriously modified. In our hypothesis, the equatorial Cu-bonded Cl atoms are constrained by the surrounding atoms whereas the axial Cl can be displaced more freely subject to the constraints of the hydrogen bonds. The symmetry of the Cu coordination would thus be approximately $4/mmm$ (D_{4h}) with the fourfold axis nearly parallel to the c axis. Our model derived by X-ray diffraction is very similar to one of the coordination models proposed for a similar compound on the basis of absorption spectroscopy measurements.³ One of the distances ($d(\text{Cu-Cl}) = 2.49 \text{ \AA}$) differs from the one proposed by the authors ($d \approx 2.2\text{-}2.3 \text{ \AA}$) whereas the other Cu-Cl distances are in accordance.

There is however another interpretation that should not be overlooked. The octahedron formed by pk(1) and pk(2) is very similar to the one formed by Cl(1) and Cl(2). Both figures can be superposed by a rotation of 12° about the a axis. In

this hypothesis, pk(1) and pk(2) would result from a disorder in the packing of the MnCl_4 layers where approximately 2% of the octahedra have an opposite tilt with respect to the normal to the layer. In view of the dimensions of the crystal ($4.8 \times 10^{-4} \text{ mm}^3$), no diffuse scattering can be expected to be observed on X-ray film even if our hypothesis is valid. Larger single-crystal specimens tend to grow with a variable Cu concentration, as observed by the changing of color under the microscope. The diffraction pattern of a reasonably large crystal would thus not be considered as representative of the structure solved in this work. On the basis of the second hypothesis being true and in view of the electron density of the Cl atoms calculated by Fourier transform of the atomic scattering factor, we can postulate that the Cu atoms are distributed among the Mn sites with the same Cl coordination. In both hypotheses however, the Cu coordination remains the same.

In view of these arguments it is understandable why only a small percentage of Cu atoms can be incorporated into a MnCl_4 framework as deduced from the phase diagram. The usual $[4 + 2]$ Cu coordination found in this type of compounds cannot be realized without perturbation of the MnCl_4 octahedra. The red color of the mixed compound originates thus very probably in the unusual octahedral coordination on the basis of absorption spectroscopy³ and X-ray diffraction.

Acknowledgment. This work was supported by the Swiss National Science Foundation (Grant No. 2.067-0.81). We wish to thank Professor D. Schwarzenbach for helpful discussions.

Registry No. $(\text{CH}_3\text{NH}_3)_2\text{MnCl}_4$, 12121-86-7; $(\text{CH}_3\text{NH}_3)_2\text{CuCl}_4$, 16950-47-3; CH_3OH , 67-56-1.

Supplementary Material Available: A listing of structure factor amplitudes (5 pages). Ordering information is given on any current masthead page.

(17) "International Tables for X-Ray Crystallography"; Kynoch Press: Birmingham, England, 1974; Vol. IV.

(18) The structure of $(\text{CH}_3\text{NH}_3)_2\text{CuCl}_4$ was determined by single-crystal diffraction to obtain the corresponding Cu-Cl distances: space group $B2_1/c$; $a = 7.276$ (1), $b = 7.380$ (1), $c = 18.654$ (2) Å; $\beta = 90.37$ (1) $^\circ$. The ammonium hydrogen atoms are linked by H bonds to two axial Cl's and one equatorial Cl with N...Cl distances from 3.29 to 3.36 Å. The space group and lattice parameters are different from those reported in ref 9.

Contribution from the Department of Chemistry,
University of Cincinnati, Cincinnati, Ohio 45221

The Chemistry of [Co]Cobalamins: Equilibrium Constants and Energies of Formation of Species in Aqueous Solution

KENNETH A. RUBINSON,* HEMAXINI V. PAREKH, EKEI ITABASHI, and HARRY B. MARK, JR.*

Received May 21, 1982

A thermochemical analysis is carried out with use of electrochemical equilibrium data derived from spectroelectrochemical experiments on aquo[Co(III)]cobalamin in aqueous solutions. The [Co(II)]cobalamin species are more stable than their corresponding Co(III) or Co(I) species in the pH range 0-11. The oxidation-reduction reaction scheme of the [Co]cobalamins is explained by the pH-dependent redox potentials of the various species. These findings and, hence, the redox properties of methylcobalamin and coenzyme B₁₂ are explained by a simple σ -orbital model. The same theoretical model also can be used to explain the electronic mechanism for photolysis of the Co-C bond as well as the low-energy limit for the cleavage. The thermal cleavage of the Co-C bond is explained as well.

The function of the B₁₂ enzymes undoubtedly depends on the fundamental chemistry of the alkyl[Co]cobalamin reaction center. Our understanding of the enzymatic processes thus requires knowledge of the equilibrium thermochemical properties, which quantitate the effects of the benzimidazole base binding, of the cobalt oxidation state, and of the cobalt-carbon bond energy. These all can be obtained in principle from electrochemical equilibrium measurements. For these, the primary requirement for determining the Co-C equilibrium bonding properties is the measurement of a reversible equilibrium potential with known products.

Toward this end, using a polarographic technique, Birke and Kim have calculated that methyl[Co(III)]cobalamin's reversible reduction potential is -1.24 V vs. SCE in neutral aqueous

solution in the presence of Triton X-100, a nonionic detergent used to prevent adsorption on the mercury electrode.¹ Coenzyme B₁₂ showed a similar value of -1.26 V . An electrochemical half-wave potential value of about -1.5 V is obtained when the methyl complex is reduced irreversibly at an Hg-Au minigrid electrode in neutral aqueous media in the absence of Triton X-100. In this case, the alkyl-cobalt bond breaks after a one-electron transfer to yield ethane and [Co(I)]cobalamin exclusively.²

(1) Birke, R.; Kim, H. *J. Electroanal. Chem. Interfacial Electrochem.*, in press.
(2) Rubinson, K. A.; Itabashi, E.; Mark, H. B., Jr. *Inorg. Chem.* **1982**, *21*, 3571-3573.

Similarly, when the methyl[Co]cobalamin is oxidized in neutral solution, a two-electron transfer occurs at approximately +0.9 V vs. SCE. The complex irreversibly breaks down to aquo[Co(III)]cobalamin and methanol exclusively.²

Further information that can be calculated from electrochemical data are the free energies of the equilibrium redox reactions of aquo[Co(III)]cobalamin, B_{12a}, and its reduction products. An understanding of the thermodynamic energies of the base coordination, protonation, and oxidation states can be obtained.

More specifically, the relative energies of formation of various [Co(I)] species are found. Since this has been put forth as a possible enzymatic intermediate, the energy required to reach this reduced state is useful in judging that possibility. In addition, due to regularities in the energies of formation of the Co-benzimidazole bond, a useful measure of the effective charge on the cobalt can be derived from the electrochemical data.

With use of a simple molecular orbital model, a significant amount of disparate chemistry of the axial ligands of the [Co]cobalamins can be rationalized to arise from the same origin. Specifically, semiquantitative agreement is found in the energies determined spectroscopically, electrochemically, and photochemically and determined from the equilibrium and rate constants associated with the axial bonding.

Reported here are the formal electrochemical potentials, E° , and the relative free energies of formation of the species of [Co]cobalamin that exist in water between pH 1 and pH 11. The results of the thermodynamic analysis of the B_{12a} redox chemistry are then used to interpret the electrochemical kinetic data and the chemistry of methyl[Co]cobalamin and coenzyme B₁₂.²

Experimental Section

The supporting electrolytes used for the spectroelectrochemical measurements were 0.5 M in KCl since there was no effect on the electrochemical potentials over the electrolyte concentration range 10–500 mM. This behavior implies that there is no association of chloride with [Co(III)]-, [Co(II)]-, or [Co(I)]cobalamin. On the other hand, binding effects, i.e., changes in E° , were seen with sodium nitrate, azide, sulfate, and thiocyanate electrolytes.

In all cases, Britton–Robinson buffer was used. The Britton–Robinson buffer, a combination of phosphate, borate, and acetate in equal measure, was found to exert a small but finite influence on the E° measured. The concentration of the buffer was accordingly kept constant between 24 and 27 mM in each ion: total acetate, borate, and phosphate. The pH was varied by adding concentrated KOH or NaOH to a stock solution before adding the buffer to the electrolyte solution.

All chemicals employed were reagent grade, and solutions were deaerated with 99.99% water-pumped nitrogen or argon. All spectroelectrochemical and cyclic voltammetric measurements were carried out with use of thin-layer cells as previously described.^{3,4}

Results and Discussion

Electrochemical Equilibria. The formal potentials, E° , were determined in this work with use of the technique of spectroelectrochemistry,³ which is well suited for the [Co]cobalamin system. This method enables one to measure the time-independent oxidation–reduction potentials as a function of pH. The method even allows the various acid–base equilibrium constants to be determined more accurately than with simple titrimetric experiments since the midpoint of the reaction need not be corrected for variations in the spectrum with pH.

The equilibrium E° values obtained as a function of pH are plotted as open circles in Figure 1. In general, the layout is similar to that previously reported by Lexa and Savéant,^{5a}

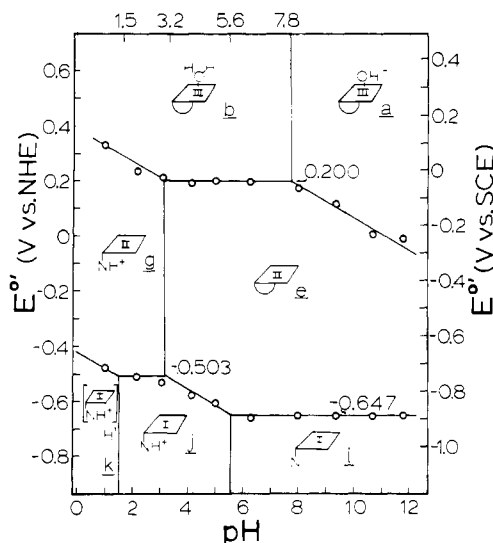


Figure 1. Results of the spectroelectrochemical equilibrium measurements. The upper set of data points are for the Co(III)/Co(II) couple, and the lower set of points are for the Co(II)/Co(I) couple. The errors in the individual data points are ± 20 mV. The lines are drawn with the assumption of a slope of 59 or 0 mV/pH unit in the appropriate pH regions. Horizontal lines are at the average value of the points along them. The vertical lines are drawn at the breaks between horizontal and sloping line segments with the important restriction that the vertical line at pH 3.2 must intersect the breaks at the same pH in both top and bottom lines.

but there are three significant differences (see below).

The diagram is, indeed, a plot of all the equilibrium constants of the system. The vertical lines are at the pK 's of the acid–base reactions, and the horizontal and sloping lines are at the Nernstian potentials of the oxidation–reduction equilibria. The chemical structures drawn represent the predominant equilibrium cobalamin species in each region. A line in the figure only represents the combination of voltage and pH where the two species symbolized on either side of that line have the same concentration.

The figure caption for Figure 1 describes some of the details of the construction of the diagram from the data points. It is worth noting here that there is little room for change in the values of the pK values since all the points of the figure are, in effect, tied together by the $pK = 3.2$ line. If the position of one of the breaks in the lines is changed, all the pK values will change since the horizontal lines at -0.647 and $+0.200$ V are fixed within a few millivolts experimentally.

Values of the Equilibrium Constants. In reference again to Figure 1, the values of the pK 's and E° and the identification of the most stable species⁶ in each of the outlined regions agrees with those of Lexa et al.⁵ with a few notable exceptions. The most important difference is that the $pK_a = 5.65$ for the free 5,6-dimethylbenzimidazole is almost a full pH unit higher than in their analysis. Our experimentally determined value falls close to the analogous 1,5,6-trimethylbenzimidazole, which is expected⁷ to have a pK_a value of 5.95–6.15 in water.⁸

(5) (a) Lexa, D.; Savéant, J. M.; Zickler, J. J. *Am. Chem. Soc.* **1977**, *99*, 2786–2790. (b) de Tacconi, N. R.; Lexa, D.; Savéant, J. M. *Ibid.* **1979**, *101*, 467–473.

(6) The arguments for the structural assignments of the species that are shown symbolically are published in the many previous papers on this subject (ref 5 and references therein). Note that the species represented can vary by an arbitrary number of neutral adducts (e.g., a water may or may not be bound axially).

(7) The pK_a for 1,5,6-trimethylbenzimidazole was measured as 5.45 in 50% ethanol–50% water.⁸ For experimentally measured pK 's of substituted benzimidazoles, the values in 50% ethanol–50% water are about 0.5–0.7 pH unit lower than in pure water.⁸ Our relatively low value of 5.6 may be a reflection of local environmental influences on the base-off benzimidazole.

(3) Heineman, W. R. *Anal. Chem.* **1978**, *50*, 390A–402A.

(4) Kenyhercz, T. M.; DeAngelis, T. P.; Norris, B. J.; Heineman, W. R.; Mark, H. B., Jr. *J. Am. Chem. Soc.* **1976**, *98*, 2469–2477.

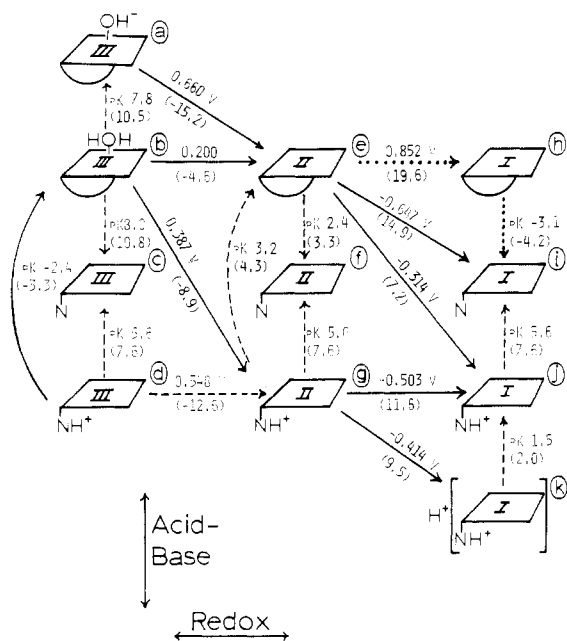


Figure 2. Free energies of interconversion (in parentheses) of the possible [Co]cobalamin species. The signs of the energies are correct for the reaction in the directions of the arrows. The free energies are standard free energies calculated at 1 atm and pH 0 (unit activity of H^+), the consistent standard state for both acid-base and oxidation-reduction (i.e., vs. NHE) processes. Solid arrows are measured values, dashed arrows are calculated values, and dotted arrows are extrapolated values. The value $pK = -2.4$ between species b and d comes from titrimetric data extrapolation by Hayward et al.¹⁰ Note that the energies of the c-f and f-i reactions have been omitted for clarity. They are assumed to be equal to those for the corresponding base-protonated species, d-g and g-j, respectively. This means we assume that the pK_a of the protonation of the unbound benzimidazole does not change along with the oxidation state of the metal.

Finally, two remaining pK 's, namely, those at pH 1.5 and 3.2, differ from those of Lexa et al.⁵ at 1.0 and 2.9, respectively. Our latter value, however, agrees exactly with that measured by EPR.⁹

Note that the structure symbol for the protonated, base-off [Co(I)]cobalamin (the species labeled h) does not show the specific mode of association of the proton. There is no chemical evidence known to us showing that the protonation occurs on one of the ring nitrogens, perhaps ring A or D where there will be a minimum of interruption of the delocalization.

Thermochemical Cycles. Two pK and E° data shown in Figure 1 can be displayed equivalently as the energies of interconversion of the species (see Figure 2). This figure shows the experimental data (solid lines), the derived data (dashed lines), and two instances of extrapolated values (dotted lines) for transformations of the species found in aqueous solution between pH 1 and pH 11. Also included are the possible intermediate species. The value of either the pK or the standard potential vs. hydrogen, E° , and the free energy, ΔG° , for each step between species are listed. The pK 's as reported are for mixed equilibrium constants. However, to the extent that the activity coefficients of the various species of cobalamin are equal, the pK 's reported here are true activity equilibrium

constants since all the interconversions are first order in each form of cobalamin.

The linear extrapolation for the two paths leading to and from species h, the hypothetical base-on form of [Co(I)]cobalamin, was made with a number of assumptions. The reasoning is as follows.

Assumption 1. The energy of protonation of base-off (unbound benzimidazole) cobalamins is the same for all oxidation states of the cobalt. Thus, the energies for $\Delta G^\circ(i \rightarrow j) = \Delta G^\circ(f \rightarrow g) = \Delta G^\circ(c \rightarrow d)$. This assumption is necessary for the calculation of all the acid-base reactions from the experimental data.

Assumption 2. The differences between base-on and base-off reduction energies are the same for $Co(III) \rightarrow Co(II)$ as for $Co(II) \rightarrow Co(I)$. Specifically, $\Delta G^\circ(b \rightarrow e) - \Delta G^\circ(d \rightarrow g) = 8.0 \text{ kcal/mol} = \Delta G^\circ(e \rightarrow h) - \Delta G^\circ(g \rightarrow j)$. From this relationship, $\Delta G^\circ(e \rightarrow h)$ is calculated.

Assumption 3. The differences in the pK values and, hence, energies of the benzimidazole base binding are linear with oxidation state. Specifically, $\Delta G^\circ(b \rightarrow c) - \Delta G^\circ(e \rightarrow f) = 7.5 \text{ kcal/mol} = \Delta G^\circ(e \rightarrow f) - \Delta G^\circ(h \rightarrow i)$. In this way the value of $\Delta G^\circ(h \rightarrow i)$ was obtained.

Note that the sum of the energies derived by using these two extrapolations yields a value close to the experimental value (14.9 and 14.4 kcal/mol, respectively). While there are numerous interrelationships between the various measured thermochemical values, there is redundancy in the measurements; e.g., the value of $\Delta G^\circ(e \rightarrow g)$ can be obtained through two independent, experimental cycles $\Delta G^\circ(e \rightarrow j \rightarrow g) = -4.4 \approx -4.3 = \Delta G^\circ(e \rightarrow b \rightarrow g)$. Thus, while this is not proof of the exactness of the extrapolated values, the values are consistent with the only related measured value, $\Delta G^\circ(e \rightarrow i)$. Further, the agreement between the extrapolated and measured values, $\Delta G^\circ(e \rightarrow h \rightarrow i) = 15.4 \text{ kcal/mol} \approx 14.9 \text{ kcal/mol} = \Delta G^\circ(e \rightarrow i)$, suggests that the behavior posited in assumption 3 is, at least, close to the true property.

As can be seen from Figure 2, the pK values of the binding of the benzimidazole to the cobalt center decreases regularly with a decrease in formal charge of the cobalt. Thus, the pK 's of the benzimidazole binding appear to provide a reasonable internal measure of that formal charge. The pK of benzimidazole binding to Co(II) is 3.2, and those for the alkyl-[Co]cobalamins are both nearly the same (methyl, 2.9; coenzyme, 3.4).¹¹ Thus, the effective charge on the cobalt when bound to an alkyl carbon is the same as when the formal charge is 2+. This conclusion is valid as long as we can neglect any effect of water binding on the cobalt centers in the Co(III) and (possibly) Co(II) species.

Relative Free Energies of Formation. We can compute free energies of formation relative to that of the species g, the protonated, base-off form of [Co(II)]cobalamin; i.e., the free energy of formation of species g is arbitrarily set equal to zero. From the energies of reaction shown in Figure 3 and the pH dependence determined from the data of Figure 1, a self-consistent set of free energies of formation can be calculated at all pH values. These are illustrated in Figure 3.

Relation of ΔG° to Other Energies. In the following discussion, we allude to both the bonding energy due to the formation of molecular orbitals and the thermodynamic free energy of various reactions at the axial positions. The corrinoid ligand appears to bind in such a way that the spectroscopic energy changes correspond with the bonding stabilities of the axial ligands.¹³ The effects due to the solvent appear to be

(8) (a) Hofmann, K. "Imidazole"; Interscience: New York, 1953; Part I, Chapter 8. (b) Davis, M. T.; Mamalis, P.; Petrov, V.; Sturgeon, B. J. *J. Pharm. Pharmacol.* **1951**, *3*, 420-430.
 (9) Bayston, J. H.; Looney, F. D.; Pilbrow, J. R.; Winfield, M. E. *Biochemistry* **1970**, *9*, 2164-2172.
 (10) Hayward, G. C.; Hill, H. A. O.; Pratt, J. M.; Vanston, N. J.; Williams, R. J. P. *J. Chem. Soc.* **1965**, 6485-6493.

(11) Pratt, J. M. "Inorganic Chemistry of Vitamin B₁₂"; Academic Press: London, 1972; Table 8.7.

(12) As seen in Figure 2, although the pK between the states h and j is 8.8, h does not form since i is more stable at all pHs. There is then no pK break in Figure 1.

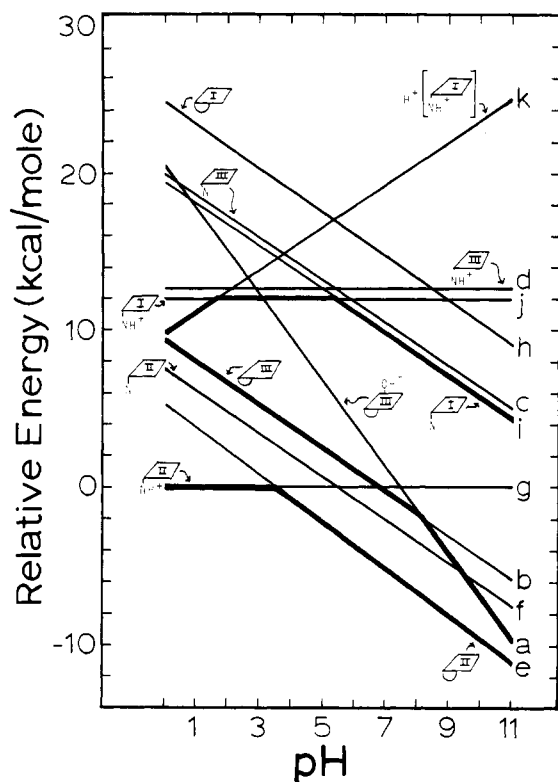


Figure 3. Relative free energies of formation vs. pH of the possible species of aquo[Co]cobalamin. Each line is labeled with the corresponding letter from Figure 2 and a symbol of the species. The heavy lines represent the free energy of the dominant species of each oxidation state. Note that the breaks occur at the pK values of each of the forms: 1.5 and 5.6 for Co(I),¹² 7.8 for Co(III), and 3.2 for Co(II).

constant or to be changing monotonically with the spectroscopic energies. In a thermochemical study, Thusius showed¹⁴ that for the equilibrium and rate constants of substitution the entropic contribution was small in comparison to the enthalpic effects. Also, he concluded that the transition state for substitution is essentially complete dissociation. In addition, the cobalt(III) in the corrinoid complex is far more labile than in other cobalt complexes, equivalent to a ΔH^\ddagger about 10 kcal/mol lower than usual.¹⁴ This is in remarkable agreement with the estimated change in the d_{z^2} orbital energy due to the very strong σ -bonding effects of the corrin ring.¹³ It appears that the combined effects of the ring bonding and crowded steric conditions around the metal cause the simple correlation between the relatively weak ligand binding, fast exchange rates, spectroscopic energies, and electrochemical potentials. We thus feel free to use the reaction free energy trends interchangeably with the changes in the binding energies found from molecular orbital formation.

Bonding Scheme To Explain the Electrochemistry Results.

The electrochemical experiments have revealed three main facts that need to be observed in any useful model for the axial bonding in [Co]cobalamin.

(1) Equilibrium reduction potentials for the Co(III)/Co(II) couple become more negative the greater the σ -donating strength of the ligands.

(2) Irreversible oxidation of methyl[Co]cobalamin occurs through a two-electron process followed by decomposition to yield aquo[Co(III)]cobalamin and methanol.

(3) Irreversible reduction of methyl[Co]cobalamin occurs through a one-electron process followed by decomposition to yield [Co(I)]cobalamin and ethane.

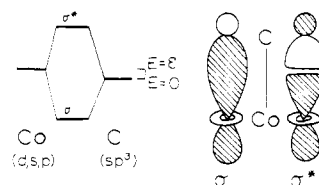


Figure 4. Diagram showing the molecular orbitals and the energy level diagram with definitions.

In addition, other pertinent experiments have shown the following.

(4) Photolysis of methylcobalamin occurs with facility from the UV region to at least 570 nm ($17\,500\text{ cm}^{-1}$ or 2.2 eV).¹⁵

(5) With use of [Co]cobalamins, nonenzymatic analogue reactions proceed with carbon skeletal rearrangements of the type seen in the biological enzyme systems. These have been done with thermal activation in the dark¹⁶⁻¹⁸ as well as with light activation.^{19,20} We first will explain, qualitatively, the effective formal charge of the cobalt and then show how the model we propose also explains the results of the irreversible oxidation and reduction of methylcobalamin as well as the photolytic and thermally activated reactions.

We recognize that the model is oversimplified. However, it does offer a coherent explanation of the chemical reactions of the [Co]cobalamins. Salem has shown that such a simplified formalism is an adequate representation of the bonding such as is found here.²¹ This is especially true insofar as the Co-alkyl center is apparently chemically isolated²² and nearly surrounded by the ring and side chains of the cobalamin ligand.²³

As noted by early workers in the field, the axial ligands exhibit a trans effect in binding.²⁴ Depending on the upper axial ligand, the 5,6-dimethylbenzimidazole bonding free energy differs by about 5 pH units.¹¹ This is equivalent to about 5 kcal/mol. Under the same conditions, the free energy of the redox reactions of cobalt varies by more than 1.5 eV, equivalent to about 37 kcal/mol. (E.g., methyl- and aquo-cobalamin at low pH have potentials at about -1 and $+0.5$ V (d \rightarrow g), respectively.) We thus make an important, simplifying assumption: In oxidation-reduction reactions involving the axial ligand of [Co]cobalamins, we can neglect the contribution of the benzimidazole binding to the free energy of the process.

We assume that for the axial ligands the σ bonding is the only important component energetically in the metal-ligand interaction, particularly that involving an alkyl carbon. The cobalt axial orbital (d, s, p mixture of A symmetry in C_{4v}) together with the ligand atomic orbital will give rise to a single bonding and antibonding orbital pair as illustrated in Figure 4. Suggestions for such a simple model were made previously by Seki et al.²⁵

(15) Taylor, R. T.; Smucker, L.; Hanna, M. L.; Gill, G. *Arch. Biochem. Biophys.* **1973**, *156*, 521-533.

(16) Dowd, P.; Trivedi, B. K.; Shapiro, M.; Marwaha, L. K. *J. Am. Chem. Soc.* **1976**, *98*, 7875-7877.

(17) Dowd, P.; Shapiro, M. *J. Am. Chem. Soc.* **1976**, *98*, 3724-3725.

(18) Scott, A. I.; Hansen, J. B.; Chung, S.-K. *J. Chem. Soc., Chem. Commun.* **1980**, 388-389.

(19) Hartshorn, A. J.; Johnson, A. W.; Kennedy, S. M.; Lappert, M. F.; MacQuitty, J. J. *J. Chem. Soc., Chem. Commun.* **1978**, 643-644.

(20) Rudakova, I. P.; Ershova, T. E.; Velikov, A. B.; Yurkevich, A. M. *J. Chem. Soc., Chem. Commun.* **1978**, 592-593.

(21) Salem, L. *Nouv. J. Chim.* **1978**, *2*, 555-562.

(22) Rubinson, K. A.; Caja, J.; Hurst, R. W.; Itabashi, E.; Kenyhercz, W. R.; Heineman, W. R.; Mark, H. B., Jr. *J. Chem. Soc., Chem. Commun.* **1980**, 47-48.

(23) Lenhert, P. G. *Proc. R. Soc. London, Ser. A* **1968**, *303*, 45-84.

(24) Hill, H. A. O.; Pratt, J. M.; Williams, R. J. P. *Chem. Br.* **1969**, *5*, 156-161.

(25) Seki, H.; Shida, T.; Imamura, M. *Biochem. Biophys. Acta* **1974**, *372*, 100-108.

(13) Rubinson, K. A. *J. Am. Chem. Soc.* **1979**, *101*, 6105-6110.

(14) Thusius, D. *J. Am. Chem. Soc.* **1971**, *93*, 2629-2635.

Path of Electron Transfer. For alkyl carbon ligands, we postulate that electron transfer occurs via the back lobe of the sp^3 atomic orbital on the carbon. For other ligands such as water, the transfer will occur through the symmetry-related orbital. This postulate expresses the fact that experimentally we have found no other electron-transfer pathway to the metal exists in cobalamins.²² Reduction of the metal center entails electron transfer into the σ^* orbital (see Figure 4). Oxidation results from electron transfer out of the σ orbital.

As shown in the Appendix, as the σ -bonding capabilities of the axial ligand increase, the energy between the σ and σ^* orbitals increases. Following from this, we can explain the first point of the electrochemical data. As the σ bonding becomes stronger, the σ^* orbital rises in energy, making it harder to inject the reducing electron into the σ^* orbital. Also, as the cobalt becomes harder to reduce, the cobalt's effective charge is decreased, as tested by the pK value of the benzimidazole binding. This reduction in charge with the increase in σ -bonding strength is also explained by the two-level molecular orbital scheme. The details are shown in the Appendix.

In addition, the second main point of the electrochemistry can be explained. This is the oxidation at the electrode, which we see consists of a two-electron transfer out of the bonding orbital at about +0.9 V vs. SCE, leaving the cobalt as Co(III). Since there remain no bonding electrons, the methyl group will leave as its carbocation, which, typically, will react with water as the nucleophile, producing methanol as the product.²⁶

To explain the third point of the electrochemistry—the reduction behavior—we postulated that the single electron from the electrodes does indeed go into the σ^* orbital from the electrode. At this large negative potential, a 2e transfer might be anticipated.^{4,5} The second electron transfer is unobserved. Thus, the one-electron product must be reacting relatively rapidly but reacting away from the electrode interface to form [Co(I)]cobalamin and ethane in a concerted reaction. This delay is probably due to the significant solvent reorganization required in analogy with the reduction of the methyl radical itself.³⁰

Other Implications of the Model. Salem has shown how a one-electron reduction can cause the dissociation of a σ -bonded moiety such as the isolated Co-alkyl bond.²¹ Thus, the reductive cleavage can be compared to alkyl halide reactions of the same type.² The [Co]cobalamin center can, perhaps profitably, be viewed as a good leaving group.

Salem, in addition, demonstrated that the reductive cleavage is, in essence, similar to photolytic cleavage due to charge-transfer transitions into the σ^* orbital as well as due to σ - σ^* excitations. Thus, the behavior of the photolysis chemistry also fits into this simple model. As proof of the fecundity of the approach, the behavior seen electrochemically—a one-electron transfer followed by a bond cleavage—has been demonstrated to exist for photolysis as well.³¹

If the photolysis of the methyl[Co]cobalamin and coenzyme B₁₂ is due to a σ - σ^* excitation, the theoretical model fits semiquantitatively. We know from the electrochemical reduction that the energy of the σ^* orbital is at approximately +1.0 eV. Relative to the same electrochemical standard, the

σ orbital (from which the electrons are removed upon oxidation) is at about +1 V. The splitting between the σ and σ^* orbitals is, thus, approximately 2 eV. This suggests that a photolysis of the Co-alkyl bond should be possible down to that energy (2 eV, 16 000 cm^{-1} , 625 nm), as indeed it is.¹⁵ This mechanism for the photolysis explains why the enzyme-like reaction can be excited photolytically^{19,20} with an alkyl radical being produced.

All that remains is to explain the thermal activation of the analogue chemical reactions.¹⁶⁻¹⁸ This now is also straightforward. So far, we have neglected consideration of the spin-pairing energy of the electrons. The exact value for the cobalt corrins is not known. However, cobalt complexes usually have values at about 16 000–20 000 $cm^{-1} \approx 2$ –2.5 eV.³² Again, as mentioned above, the total splitting of molecular orbital energy levels is about 2 eV. The similarity of the splitting and spin-pairing energies, while perhaps occurring merely by chance, suggests a simple mechanism for thermal, homolytic scission of the cobalt-carbon bond. This simply involves the simultaneous spin and σ - σ^* transition, which is an allowed transition thermally but not spectroscopically.

Metal Bonding and the Chemistry and Biochemistry of the Cobalamins. Earlier, we derived the relative free energies of formation over the pH range investigated. These are illustrated in Figure 3. Co(I) has been postulated to be an intermediate form in some coenzyme reactions.³³ If this is the case in fact, at neutral pH about 13 kcal/mol will have to be supplied to the cobalamin system to bring it to Co(I), that is, the free energy difference between the [Co(I)]cobalamin species and the lowest energy form of [Co(II)]cobalamin. Any further stabilization of Co(III) or Co(II) species by binding with an axial ligating group will reduce the probability of formation of Co(I) even more since the Co(I) will not be axially coordinated. This is inferred from the fact that Co(I) is isoelectronic with Ni(II), which when chelated with corrin does not appear to bind any ligands in the fifth or sixth position.²²

Another interesting conclusion derives from the relative energies of the [Co(II)]cobalamin in base-on and base-off forms. The base-off form is more stable by about 3 kcal/mol. From this value we infer that, if the active form of the coenzyme has the base off in the Co(II) form,³⁴ at least 3 kcal/mol must be supplied by an interaction with some other species—protein, substrate, or solvent. In addition, the energy required places a limit on the modification that the protein can produce in coenzyme B₁₂ through the benzimidazole, or vice versa, if the environment is like that in solution.

However, the most important result found earlier is that, in the pH range 1–11, all the [Co(II)]cobalamin species are more stable than any of the Co(III) forms. This is true whether the benzimidazole base is protonated or not. Thus, the [Co(III)]cobalamins will act as moderately strong oxidizing agents.

The axial bonding position of various cobalt corrins has been observed to be highly nucleophilic. As mentioned above, the electrons added upon reduction occupy the axial orbital, mostly d_{z^2} . This orbital has a relatively high energy in comparison with that of other cobalt chelates.¹³ The higher energy level must be due to an increase in extension—an increase in the average value of $\langle r^2 \rangle$ —for the orbital. The raised orbital energy and increased orbital projection is the underlying cause of the significant nucleophilicity of [Co]corrins. Since good nucleophiles are good leaving groups, we concluded that the Co(III) in the cobalamin chelate is ready to be reduced and to act as an excellent leaving group. This is true regardless

(26) There is a possibility that the carbocation may react with one of the adjacent ring nitrogens. The properties of these have been explored in corroles and porphyrins.^{27,28} The properties are similar to those of the isomers investigated by some workers.²⁹

(27) Johnson, A. W.; Ward, D.; Elson, C. M. *J. Chem. Soc., Perkin Trans. 1* **1975**, 2076–2085.

(28) Jackson, A. H. In "The Porphyrins"; Dolphin, D., Ed.; Academic Press: New York, 1978; Vol. 1, Part A, Chapter 8.

(29) Friedrich, W.; Nordmeyer, J. P. *Z. Naturforsch. B: Anorg. Chem., Org. Chem., Biochem., Biophys., Biol.* **1969**, *24B*, 588–596.

(30) Toffel, P.; Henglein, A. *Faraday Discuss. Chem. Soc.* **1977**, *63*, 124–133.

(31) Endicott, J. F.; Ferraudi, G. J. *J. Am. Chem. Soc.* **1977**, *99*, 243–245.

(32) Cotton, F. A.; Wilkinson, G. "Advanced Inorganic Chemistry", 4th ed.; Wiley: New York, 1980; Table 20–3.

(33) Babior, B. M. *CRC Crit. Rev. Biochem.* **1979**, *6*, 35–102.

(34) Wood, J. M.; Brown, D. G. *Struct. Bonding (Berlin)* **1972**, *11*, 41–105.

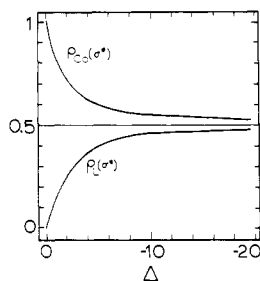


Figure 5. Graph of the values of the orbital coefficients as they vary with Δ . $\rho_{Co}(\sigma^*) = \rho_L(\sigma)$ and $\rho_L(\sigma^*) = \rho_{Co}(\sigma)$ in the absence of overlap. The values were calculated as in ref 13.

of the state of the benzimidazole.

Acknowledgment. The authors wish to thank Edward Deutsch, Hans Jaffe, Darl McDaniel, Graham Palmer, and William Rubinson for critical reading of the manuscript. This work was supported in part by NSF Grant CHE 76-04321.

Appendix

The values of the orbital energies are found by solving the secular determinant, where β defines the generalized interaction and E the eigenvalue energies:

$$\begin{vmatrix} \epsilon - E & \beta - E \\ \beta - E & \epsilon - E \end{vmatrix} = 0$$

We assume no overlap in this model; the conclusions would be unchanged by including it.

We define $\Delta = 2\beta/\epsilon$, where ϵ is, as depicted in Figure 4, the splitting between the cobalt orbital energy and that of the bound ligand. We denote the electron density contributed by each atomic orbital that goes to make up the two molecular

orbitals by, respectively, $\rho_{Co}(\sigma)$, $\rho_L(\sigma)$, $\rho_{Co}(\sigma^*)$, and $\rho_L(\sigma^*)$. The values of the last two are shown graphically as a function of Δ in Figure 5. In the limit of no interaction, $\Delta = 0$, the molecular orbitals become atomic orbitals; $\rho_{Co}(\sigma^*) = \rho_L(\sigma) = 1$ for the system as defined in Figure 4. Further, as the value of Δ takes on larger negative values, the electrons in the orbitals tend increasingly to become equally distributed over the two atomic centers. The orbital coefficients approach 0.5, the value that defines perfect covalency of the bond.

Within the molecular orbital formalism, two ways exist to change the oxidation and reduction potentials of the [Co]cobalamins with changing axial ligation: changing the relative energy splitting between the metal and ligand atomic orbitals, ϵ , and changing the size of the bonding interaction, β . It seems reasonable to consider that the metal orbital remains at a constant energy. Thus, variation in the value of ϵ will be due only to a change in the different ligand energy levels, which are not experimentally determinable directly. The second possible variation, the magnitude of the bonding interaction, is larger for CH_3 than for H_2O due to the better σ -donor properties of the former.

The first main point of the electrochemistry, concerning the trend in reduction potentials, can be explained by a change in either ϵ or β . When the cobalt is found, experimentally, to be in a higher formal oxidation state, the theory shows that the antibonding orbital occupied as a result of the reduction must be lower in energy. Both the higher oxidation state and lower σ^* -orbital energy results if $2\beta/\epsilon$ becomes smaller. This can occur by either a decrease in β , the bonding interaction, or an increase in ϵ , the atomic orbital energy separation. Thus, the better σ donor will have a higher reduction potential and lower oxidation potential as observed experimentally.

Registry No. Aquocobalamin, 13422-52-1; methylcobalamin, 13422-55-4; coenzyme B₁₂, 13870-90-1.

Contribution from the Department of Chemistry, Purdue University, West Lafayette, Indiana 47907

Electron-Transfer Kinetics between Deprotonated-Peptide Complexes of Nickel(III) and Nickel(II)

CARL K. MURRAY and DALE W. MARGERUM*

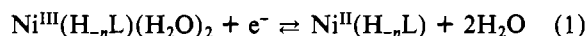
Received April 9, 1982

Cross reactions between nickel(III) peptides and nickel(II) peptides in aqueous solution are used to evaluate the self-exchange rate constants, k_{11} , of these species. The values of k_{11} for 16 different peptide complexes vary with their structure but can be classified into the following groups: triply deprotonated peptides ($1.2 \times 10^5 \text{ M}^{-1} \text{ s}^{-1}$), except for H_3G_5 ($4.2 \times 10^4 \text{ M}^{-1} \text{ s}^{-1}$), and doubly deprotonated peptides ($1.3 \times 10^4 \text{ M}^{-1} \text{ s}^{-1}$), except for α -aminoisobutyryl tripeptides ($5.5 \times 10^2 \text{ M}^{-1} \text{ s}^{-1}$). The cross reactions are catalyzed by bridging ligands with a 10-fold increase in the rate constant in the presence of $5 \times 10^{-3} \text{ M Br}^-$. The order of enhanced reactivity is $\text{Br}^- > \text{Cl}^- > \text{N}_3^-$, and there is no enhancement with F^- .

Introduction

Nickel(III)-deprotonated-peptide complexes are formed readily from the corresponding nickel(II) species by either electrochemical or chemical oxidation.^{1,2} These nickel(III) species are moderately stable in aqueous solution. Their EPR spectra^{2,3} and electrochemical behavior⁴ are consistent with a tetragonally distorted octahedral structure with two water molecules in the axial sites and the unpaired electron in the metal d_{z^2} orbital. Nitrogen ligands such as pyridine or am-

monia have been shown to form axial adducts with nickel(III) peptides.^{3,5} On the other hand, the nickel(II) peptides are d^8 , square-planar species^{4,6} with no axial solvation. Thus, reduction of nickel(III) peptides is accompanied by a release of coordinated water molecules in accord with eq 1, where L



is the peptide ligand and n is the number of deprotonated peptide or amide nitrogens in the complex. The $\text{Ni}^{\text{III,II}}$ reduction potentials vary from 0.79 to almost 0.9 V vs. the normal hydrogen electrode, depending on the nature of the

(1) Bossu, F. P.; Margerum, D. W. *J. Am. Chem. Soc.* **1976**, *98*, 4003.

(2) Bossu, F. P.; Margerum, D. W. *Inorg. Chem.* **1977**, *16*, 1210.

(3) Lappin, A. G.; Murray, C. K.; Margerum, D. W. *Inorg. Chem.* **1978**, *17*, 1630.

(4) Youngblood, M. P.; Margerum, D. W. *Inorg. Chem.* **1980**, *19*, 3068-3072.

(5) Murray, C. K.; Margerum, D. W. *Inorg. Chem.* **1982**, *21*, 3501-3506.

(6) Margerum, D. W.; Dukes, G. R. *Met. Ions. Biol. Syst.* **1974**, *1*, Chapter 5.